JOURNAL OF BACTERIOLOGY, July 1992, p. 4798–4806
0021-9193/92/144798-09$02.00/0

Vol. 174, No. 14

Molecular Modelling of the Three-Dimensional Structure and Conformational Flexibility of Bacterial Lipopolysaccharide

MANFRED KASTOWSKY,* THOMAS GUTBERLET, AND HANS BRADACZEK

Institut für Kristallographie der Freien Universität Berlin, Takustrasse 6, W-1000 Berlin 33, Germany

Received 22 November 1991/Accepted 27 April 1992

Molecular modelling techniques have been applied to calculate the three-dimensional architecture and the conformational flexibility of a complete bacterial S-form lipopolysaccharide (LPS) consisting of a hexaacyl lipid A identical to *Escherichia coli* lipid A, a complete *Salmonella typhimurium* core oligosaccharide portion, and four repeating units of the *Salmonella* serogroup B O-specific chain. X-ray powder diffraction experiments on dried samples of LPS were carried out to obtain information on the dimensions of the various LPS partial structures. Up to the Ra-LPS structure, the calculated model dimensions were in good agreement with experimental data and were 2.4 nm for lipid A, 2.8 nm for Re-LPS, 3.5 nm for Rd-LPS, and 4.4 nm for Ra-LPS. The maximum length of a stretched S-form LPS model bearing four repeating units was evaluated to be 9.6 nm; however, energetically favored LPS conformations showed the O-specific chain bent with respect to the Ra-LPS portion and significantly smaller dimensions (about 5.0 to 5.5 nm). According to the calculations, the Ra-LPS moiety has an approximately cylindrical shape and is conformationally well defined, in contrast to the O-specific chain, which was found to be the most flexible portion within the molecule.

Lipopolysaccharides (LPSs) are macromolecular amphiphiles that are present exclusively in the outer leaflet of the outer membrane of gram-negative bacteria. LPSs are anchored in the outer membrane by their lipid A component, and their polysaccharide chain is presented at the cell surface (Fig. 1). Thus, LPSs not only are involved in membrane functions essential for the survival of the bacterium (e.g., the formation of an effective permeation barrier to harmful substances) but also play an important role in a number of recognition processes of the host's defense system, which may invoke antibodies against the LPS surface structures (28, 30). Since purified LPSs obtained from bacteria induce toxic effects, they are likely to represent important factors in gram-negative infections; therefore, LPSs are also called endotoxins (42). LPSs from different bacteria generally differ in chemical composition. However, for some strains the detailed chemical structures of LPSs have been established (3, 10, 19). More recently, the three-dimensional architectures of the three main LPS regions, i.e., the lipid part (13), the core oligosaccharide (11), and the O-specific chain (2), were studied by molecular modelling techniques and several different experimental methods. Most recently, the crystal structure of a *Salmonella* O-antigen dodecasaccharide-Fab complex was reported (6). In this study, for the first time, the three-dimensional structure of a complete S-form bacterial LPS, as predicted by molecular modelling, is presented. The statistical Monte Carlo modelling method was used to estimate the flexibility of the LPS oligosaccharide portion. X-ray powder diffraction experiments were performed to measure the molecular dimensions of partial LPS structures.

MATERIALS AND METHODS

Primary chemical structure of the calculated LPS model. The model structure is composed of LPS components from two different bacteria: the lipid part is from *Escherichia coli* (13, 44), the core oligosaccharide is from *Salmonella typhimurium* (11), and the O-specific chain is characteristic for *Salmonella* species of serogroup B (2). However, since the *E. coli* lipid A structure was identified in *S. typhimurium* LPS (27) and since the hexaacyl lipid A component of *Salmonella minnesota*, representing the major lipid component, was shown to be identical to the *E. coli* lipid A structure (28), one might call the model considered here *Salmonella* LPS. A detailed scheme showing the substitution pattern used in the calculations is given in Fig. 2.

Molecular modelling methods. The choice of a method for evaluating conformational energies depends upon the size of the structure, i.e., the number of degrees of freedom to be investigated. In general, empirical methods have been chosen for conformational analyses in large oligosaccharides (1, 13, 22, 24). The modelling programs used in this study were GESA (geometry of saccharides) (1, 22) and CEC (conformational energy calculations) (12). The CEC program uses the ECEPP (empirical conformation energy program for peptides) force field, which was demonstrated to be applicable to saccharides as well as to proteins (13, 18, 26, 36, 43). Both programs have provisions to account for the exoanomeric effect (38). In CEC, a Monte Carlo routine (9, 21), which allows an estimation of the conformational flexibility, is implemented (9). In all calculations with GESA or CEC, partial atomic charges were ignored. A more sophisticated, very computer-time-demanding approach would require the simulation of numerous solvent molecules and interspersed cations to balance charges (31, 39), so it appears acceptable, in a first attempt, just to account for the steric requirements within the LPS models.

Starting geometries for the three LPS main regions. The conformations of the LPS lipid part have been studied in great detail. The data obtained for the hexaacyl *E. coli* lipid A (13) correspond well to those of other studies on the heptaacyl lipid A component of *S. minnesota* LPS (16, 29); i.e., both molecules show the lipid A diglucosamine backbone tilted against the membrane normal by approximately 50°, and both have tightly packed acyl chain arrangements. The *E. coli* Re-LPS, composed of lipid A and a 2-keto-3-deoxy-D-mannooctonic acid (KDO) dimer, has been mod-

* Corresponding author.

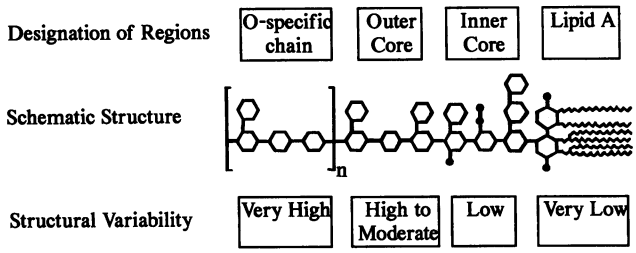

FIG. 1. Schematic representation of the general architecture of enterobacterial LPS (28). Saccharides are depicted as hexagons, acyls chains are shown as wavy lines, and phosphate and 2-aminoethylphosphate groups are shown as filled circles. One O-specific chain repeating unit is indicated in brackets.

elled (13). The lowest-energy *E. coli* Re-LPS conformation (13) was chosen, and a third KDO moiety was attached in analogy to the starting geometry for the KDO dimer. For the rest of the core oligosaccharide moiety, an *S. typhimurium* model data set was prepared as described recently (11). This data set was modified by adding the missing phosphate and 2-aminoethylphosphate groups. A model of the *Salmonella* serogroup B O-specific chain was constructed from data reported previously (2). Four repeating units were constructed.

In all calculations of the complete LPS molecule, the mature lipid A component, except for the two phosphate groups of the lipid A diglucosamine backbone, was kept fixed. All other rotations around single bonds of the rest of the LPS model were treated as variables (i.e., the complete LPS model has 187 free axes).

X-ray powder diffraction experiments. Self-assembled LPS samples with multiple bilayers were prepared as follows. To lyophilized LPS (0.2 mg), 50 μl of water (distilled three times) was added, and the mixture was shaken and ultrasonified (10 min). Droplets (5 μl) were then placed side by side on the polished, hydrophobic side of a silicon wafer (a kind gift of Wacker Chemie, Burghausen, Germany). After the droplets dried, new droplets were spread out on the previously generated spots to mount an extended drop covering an area of ~5 by 10 mm. This drop was allowed to dry in the air. LPS (for *S. minnesota*, lipid A of the Re mutant strain R595, Re-LPS of strain R595, Rd-LPS of strain R7, and Rc-LPS of strain R5; for *S. typhimurium*, Rc-LPS of strain SL684 and Ra-LPS of strain TV119) was purchased from Sigma Chemie (Deisenhofen, Germany) and used without further purification. X-ray diffraction was performed with a Phillips powder diffractometer. Data were collected with a proportional counter by the conventional $\Theta - 2\Theta$ method. The monochromator was adjusted to the Cu-K_α wavelength of 0.15405 nm. Double-layer spacings (d) were calculated by using Bragg's equation, $n \times \lambda = 2 \times d \times \sin(\Theta)$, where n denotes the order of reflection and 2Θ equals the scattering angle. Errors were estimated from variations of the 2Θ peak-to-peak distances.

RESULTS

The results presented below focus on the overall structural features of the model. Some important details, especially of the main chain glycosidic linkages, are reported first. Then the conformational flexibilities along the oligosaccharide main chain and the molecular dimensions are presented.

Linkage of KDO I to lipid A. In a previous study (13) it was shown that there are only two main arrangements of the KDO dimer with respect to lipid A. In the first type of arrangement, the KDO I carboxyl group may approach the GlcN II phosphate group, resulting in chelatelike geometries, which are favorable in complexing divalent cations (8). The other type of KDO arrangement is characterized by hydrogen bonds from the C-7 or C-8 hydroxyl group of the KDO II to the phosphate group attached to the GlcN I residue of the lipid A moiety. In the present study, the latter type of arrangement was found to be preferred for the complete LPS molecule. Other orientations of the inner core KDO I lead to a sharp bending directly at the linkage of lipid A to inner core; in some cases, this causes the outer core portion to point back into the hydrophobic domain. Thus, it seems reasonable not to favor such conformations for the complete LPS model (14). However, care must be taken when partial core structures, for which a slight bending is acceptable, are considered. Partial core structures may differ in conformation from the complete LPS molecule.

A substituent in position 4 of KDO I is critical for the Hep-KDO linkage conformation. The Hep-KDO linkage (Hep is L-*glycero*-D-*manno*-heptose) is unique within the LPS molecule with respect to the fact that the linkage oxygen is oriented axially relative to both the reducing and the nonreducing sugars. For such an axial-axial linkage type, only a few reference structures are available in the Cambridge Structural Database (5). However, in this source the crystal structure of D-Gal-α(1→4)-D-Gal closely resembles the Hep-KDO moiety. The Gal-Gal linkage conformation is ruled by a hydrogen bond between O-3–H-3 and O-5′ (37). Consequently, a similar arrangement was calculated for an isolated Hep-KDO dimer. Such a hydrogen bond, however, cannot be formed if KDO I is substituted at the 4 position, which is equivalent to the Gal-3 position because of the shifted numbering in KDO. As a result, another linkage conformation type (35) was found for the Hep-KDO-KDO trisaccharide. In the calculated complete LPS models the (core-)Hep-KDO linkage has a strong impact on the direction in which the core protrudes; thus, it appears important that the C-4 position of KDO I is blocked by being substituted by another KDO or other groups.

The inner core forms a densely packed moiety. Although in the calculated LPS model the Hep I residue carries a bulky 2-aminoethylpyrophosphate group, the prefered linkage conformation of the Hep I-Hep II moiety showed only slight deviations from that of the unsubstituted disaccharide. Our own calculations revealed that the arrangement of the heptose part of the inner core is very similar to that reported in the literature (11), for which phosphates were not taken into consideration. It should be noted that the overall shape of the inner core was strongly anisotropic (i.e., the inner core forms an entity approximately 0.8 nm high and 1.6 nm wide). The densely packed sugars of the inner core and the phosphate groups indicate a calculated enormous partial density of 1.51 to 1.56 g/cm^3.

Outer core pentasaccharide. Because of the α(1→3) and α(1→2) linkages, the outer core was reported to form one loop of a left-handed helix with a repeating unit of about four glycosyl residues (11). The arrangement appears to be very shallow, so that the *N*-acetyl group of the GlcNAc residue comes in close contact with the Gal II residue. Our calculations with the CEC program indicated a slight energetic preference for a right-handed outer core arrangement in the absence of the *N*-acetyl group of GlcNAc, whereas the GESA calculations always showed a preference for left-handed arrangements. In the presence of the *N*-acetyl group, both programs yielded similar results, so this has no bearing

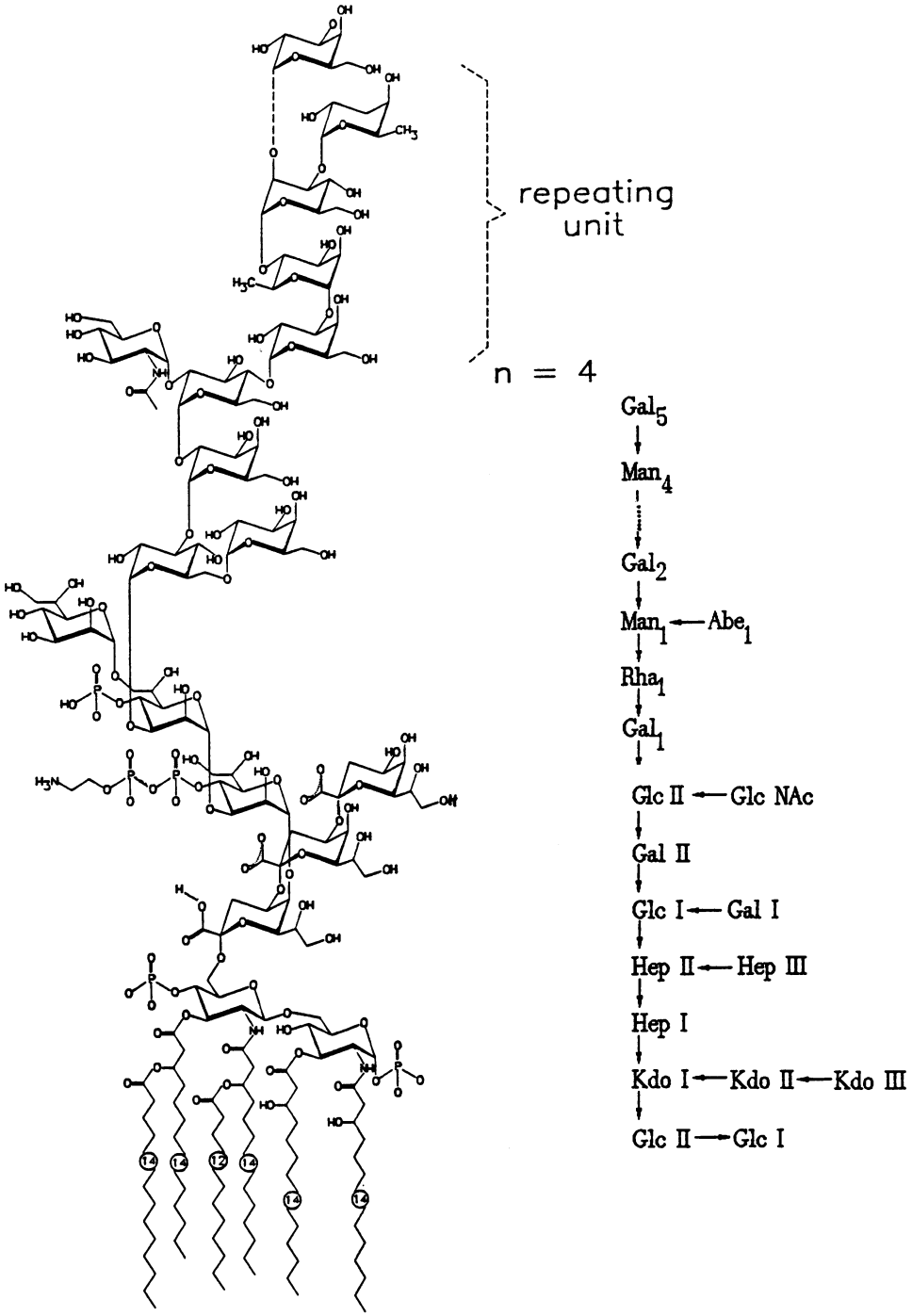

FIG. 2. Chemical structure of the LPS model used in the calculations. The O-specific chain consists of four identical repeating units and a terminal Gal residue. Note that a hexaacyl lipid A component is used and that the two main chain heptoses are substituted in position 4 by phosphate and 2-aminoethylpyrophosphate, respectively. On the right the designations of each of the saccharide residues are given.

for the calculated outer core structure, but it demonstrates that the *N*-acetyl group is of some importance to the actual conformation of the outer core.

Different side views of an LPS model (Fig. 3 and Fig. 4) show similar outlines for lipid A and the inner core (i.e., the smaller and the longer sides coincide). The outer core is oriented in such a way that its smaller side appears to be rotated about 90° with respect to lipid A and the inner core. This specific orientation generates an apparent partitioning between the inner and the outer cores (11).

Linkage of the O-specific chain to the core oligosaccharide. The O-specific chain is attached to the core oligosaccharide via the Gal-α(1→4)-Glc II linkage. Since the attachment site of the O-specific chain turned out to be located at the outermost and free end of the outer core, there seem to be no steric hindrances directing the O-specific chain in any spe-

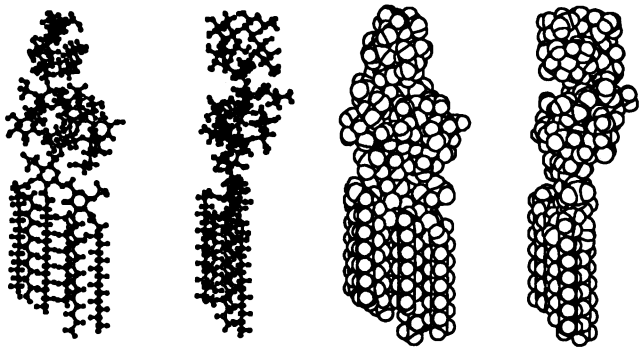

FIG. 3. Ball-stick and space-filling models of the Ra-LPS fragment of the calculated structure. The lipid A, inner core, and outer core each form compact segments. The anisotropic shape of the inner core is similar to that of the lipid A component. The smaller side of the outer core appears to be rotated about 90° with respect to the smaller side of the inner core, thus generating an apparent separation between the inner and outer core portions.

cific way. This would mean that the intrinsic properties of the glycosidic linkage determine the overall orientation of the O-specific chain. Nevertheless, the conformations of the Gal-Glc linkage were recognized to be limited to some extent by close approach of both of the C-6 hydroxymethyl groups of the saccharide. Therefore, we conclude that any increased flexibility of the O-specific chain cannot totally be attributed to the linkage of the core to the O-specific chain but must be a property of the O-specific chain itself (see below). In this context it should be noted that the most extended form of the LPS model (Fig. 4), which was obtained by application of a stretching potential between the outermost parts of the molecule, was found to be energetically disfavored, partly because of short contacts at the linkage of the core to the O-specific chain. In contrast, the energetically favored conformations of the complete LPS model showed a bent O-specific chain (Fig. 5).

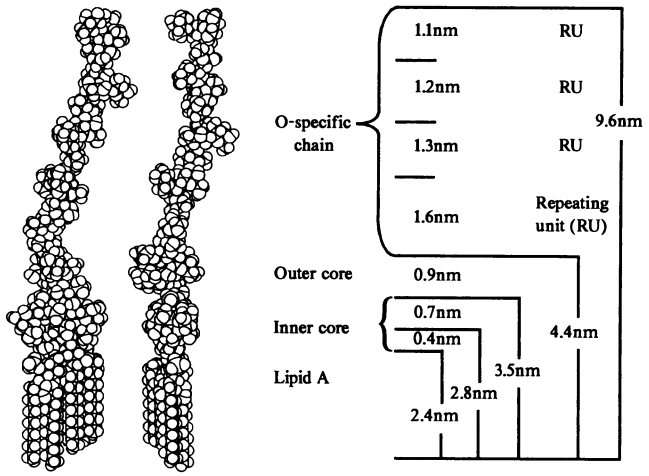

FIG. 4. Dimensions of the calculated LPS model and of partial structures. The conformer depicted shows the O-antigenic chain in its most stretched form. The length of the O-antigenic chain is an upper limit, whereas dimensions for other molecular portions are typical values. The dimensions of partial LPS structures up to the Ra-LPS structure (including the outer core) fit quite well with experimental data.

Flexibility within the oligosaccharide portion of the calculated LPS model. Up to now, long-chain (S-form) LPS, especially the O-specific chain, has frequently been sketched as a linear, rodlike strand (20). More recent schemes show a heavily coiled O-specific chain (16, 28, 32). However, it is clear that an oligosaccharide chain consisting of identical repeating units is consistent with a heavily coiled arrangement only if it has such a high flexibility that bending can occur; a totally stiff oligosaccharide chain would be better described by more highly ordered structures like helices. Thus, an estimate of the flexibility of the LPS oligosaccharide portion is of great interest. To address this problem, we carried out several Monte Carlo simulations. The Monte Carlo procedure can be described as follows. As stated in Materials and Methods, the LPS molecule has 187 free axes. During a Monte Carlo simulation, small random rotations around these axes are generated (i.e., small conformational changes are induced). Depending on the conformational energy, the generated conformations are accepted or rejected, and another trial is initiated (21). This generates a series of conformations that might be considered as snapshots of a moving molecule (Fig. 6). By monitoring the rotations around individual axes, it is possible to quantitate the conformational flexibility at any site within the molecule.

Inspection of the flexibilities of all glycosidic linkages within the molecule revealed that the LPS inner core region is rather rigid compared with the O-specific chain. The outer core portion showed intermediate flexibility. Exceptions can be found for the side chain saccharides within the inner and outer cores. Within the O-specific chain, the Rha-Gal and Gal-Man linkages were found to be the most flexible linkages, with ψ angles showing an enormous range of possible values. Similar findings are reported in the literature for the Rha-Gal (2) and the Gal-Man (6) linkages.

Molecular dimensions of partial LPS structures as obtained from X-ray powder diffraction experiments. Assuming that LPS molecules, integrated in a lamellar, bilayered arrangement, are not tilted or are only slightly tilted against the membrane normal, the relationship of the bilayer spacing (d) to the molecular extension (L) along the membrane normal is expressed as $L = d/2$. Of course, this only holds true for unswollen (i.e., not or only poorly hydrated) samples (23). A number of studies on LPS bilayer spacings have been reported in the literature. We carried out a series of X-ray powder diffraction experiments to obtain dimensions of bacterial LPSs that have chemical compositions close to that of the calculated model (Table 1).

In the X-ray diffraction patterns of the various LPS samples, three to five orders of reflection could be indexed unambiguously, clearly establishing the bilayered structure of the samples. For lipid A and Re-LPS, the first-order reflection is accompanied by only very small higher-order reflections; in contrast, the second-order reflections were significantly more intense in longer LPS structures. This finding is in agreement with the assumption that the head group regions of these LPSs are enlarged compared with those of lipid A and Re-LPS.

It should be noted that besides the chemical heterogeneity of the LPS samples, the bilayer spacings generally depend on the degree of hydration, temperature, and ion content of the samples (33). The water content of our dried samples was not measured but is probably very low. This is indicated by the fact that the respective entries in Table 1 are close to the minimum values, i.e., close to the unswollen bilayer dimensions (23). Therefore, we conclude that such data are fair measures of molecular dimensions.

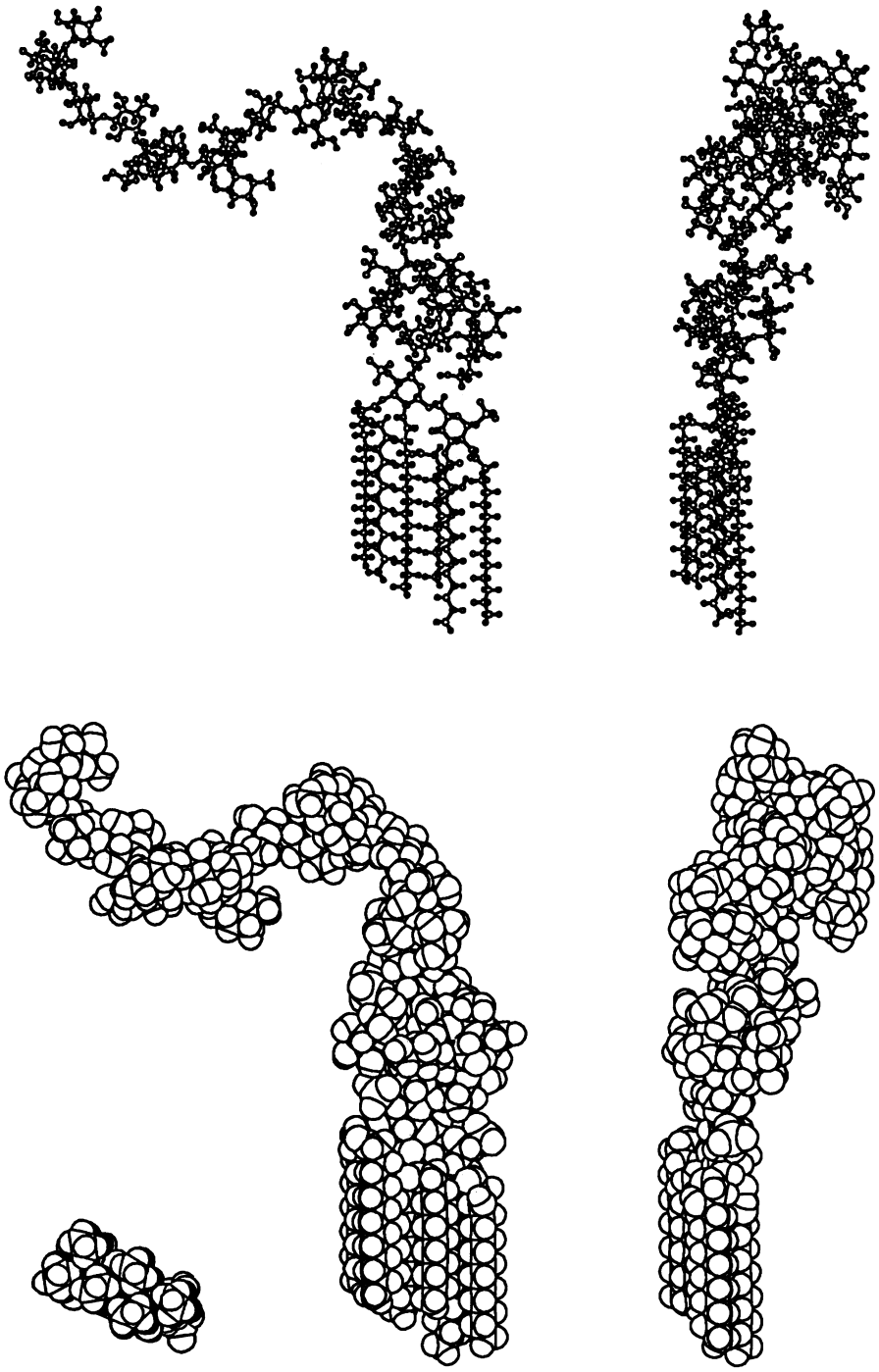

FIG. 5. Side views of an energetically favorable S-form LPS conformer showing the O-specific chain at an almost right angle with respect to the membrane normal. In a membrane arrangement, the O-antigenic chain would lie flat on top of the head groups of neighbor molecules. The acyl chain ends of a truncated molecule are shown on the bottom left.

It should be noted that the Rc-LPS core oligosaccharide portion of *S. minnesota* differs from that of *S. typhimurium* (i.e., the model structure); it lacks the outer core Gal I residue, and the substitutions of the inner core region may differ (4). However, all of the lipid A and Re-LPS structures should be comparable to those of the calculated model. Also, the experimentally established trends in differences in dimensions for partial LPS structures should correspond to the respective differences within the calculated structure.

Dimensions of the calculated LPS model. In Fig. 4, side views of a complete, fully stretched S-form LPS model are given. This conformation was chosen for clearness of representation. It has to be stressed that this stretched conformation shows typical dimensions up to the Ra-LPS structure.

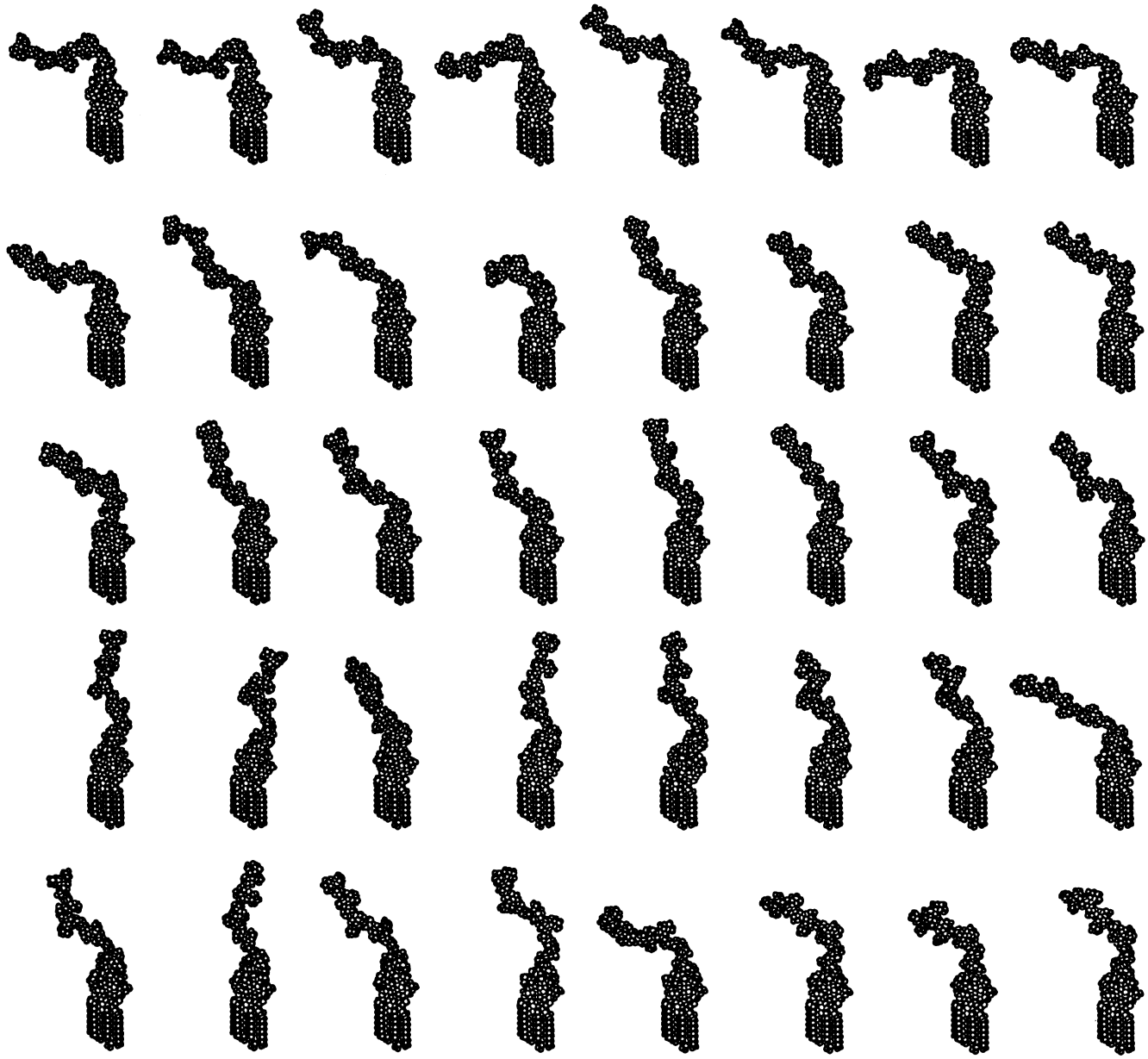

FIG. 6. Selected snapshots of S-form LPS conformers generated during a Monte Carlo run; 404,700 conformers were generated in total, and each 10,000th was selected. The Monte Carlo run was initiated from the energetically favored conformation depicted in Fig. 5. Note that the O-antigenic chain is no regular helix over longer chain distances and simulation periods and can be found in stretched or bent orientations, whereas the LPS portions up to the Ra structure are almost conserved in conformation.

The dimensions shown in Fig. 4 are approximate values, since it is not easy to define the beginnings and ends of the partial LPS structures. However, it was decided to define the baseline of the models at a position midway between the acyl chain tails, which end at different levels. This choice is justified by experimental data indicating that the acyl chains interdigitate to some extent (17).

According to Fig. 4, the lengths of the lipid A and Re-LPS parts were calculated to be approximately 2.4 and 2.8 nm, respectively. The small increase in length (only 0.4 nm) caused by the KDO portion is backed by three independent X-ray experiments (Table 1). As mentioned above, the inner core is densely packed, and it is obvious that the increase in length from Re-LPS to Rd-LPS (about 0.7 nm) is again very small. The Rc-LPS structure differs from the Rd-LPS structure by one Glc residue. However, since this Glc residue is embedded within the outer core of the calculated LPS model, there is no clear boundary between Rd-LPS and Rc-LPS structures. The increase in length from Rd-LPS to Rc-LPS was therefore estimated to be at least 0.2 nm and at most 0.5 nm. The complete outer core contributes ~0.9 nm, and each repeating unit of the O-specific chain, in its most extended conformation, adds about 1.1 to 1.6 nm to the length of the LPS model. The most extended model conformer with four repeating units is 9.6 nm long; however, in the energetically favored model with a bent O-specific

TABLE 1. Dimensions of bacterial LPSs with structures comparable to that of the calculated model

Species or model	Dimensions (L, nm)[a] of bacterial LPSs						References or source
	Lipid A	Re-LPS	Rd-LPS	Rc-LPS	Ra-LPS	S-form LPS	
Escherichia coli	2.30	2.74					40
	2.55						33
					4.38		15
Salmonella minnesota	2.28	2.72					40
		3.20	3.60				33
		2.93			4.24		15
	2.60	3.00				5.60	23
		2.70				5.45	41
	2.32–2.38	2.85–2.95	3.25–3.35	3.40–3.50			This study
Salmonella typhimurium				3.65–3.75	4.20–4.40		This study
Salmonella model	2.40	2.80	3.50	3.70–4.00	4.40	9.60[b]	Calculated

[a] Molecular extensions (L) are assumed to be related to the X-ray bilayer periodicities (d) by $L = d/2$.
[b] Dimension of the model with the O-antigenic chain in its most stretched conformation.

chain, the size of the LPS is in the range of 5.0 to 5.5 nm (Fig. 5).

The dimensions of the calculated model are in reasonable agreement with our experimental data for *S. typhimurium* LPS and with other data given in Table 1, except for the *S. minnesota* Rd-LPS and Rc-LPS structures, for which the dimensions are significantly smaller than those of the model. This finding must be due to structural variations in the inner core regions of the *S. minnesota* Rd-LPS and Rc-LPS samples as compared with the modelled structure. It is most probable that some of the heptoses and other substituents are missing in such LPSs (3, 4, 28).

In conclusion, up to the Ra structure, the model dimensions fit quite well to experimental data; thus, the calculated model seems to be validated. However, it should be pointed out that models with slightly different conformations (e.g., with alternative Hep III orientations) or even with slight compositional variations (e.g., lack of Hep III) may produce molecular dimensions similar to those of the calculated structure. This means that none of the proposed LPS model conformations is proven, but the good agreement of the theoretical model with experimental data leads us to feel confident that the calculated overall architecture is correct. Therefore, we believe that the proposed models, at least up to the Ra structure, are valuable working models.

DISCUSSION

Molecular modelling techniques were applied to calculate the three-dimensional architecture and conformational flexibility of a complete bacterial S-form LPS. In addition to theoretical calculations, molecular dimensions of partial LPS structures were evaluated from X-ray powder diffraction data. With these methods, one can expect to get detailed structural model information. However, as is the case with any theoretical model, there are some assumptions that can limit the transferability of the calculations to real situations.

Because of the size of the molecule, the calculations had to be restricted to a single, uncharged, nonhydrated, and partially rigid molecule. It could be argued that ignoring charges is the most serious simplification, since in the inner core charges may have important consequences. Therefore, it is evident that the calculated LPS model is a working model that has to be checked against further experimental data.

In this study, we chose a specific LPS primary chemical structure. However, the three main subunits of the calculated model follow general patterns, so that the exchange of any of the subunits by another one with a different primary chemical structure would not necessarily lead to a totally different spatial arrangement. For example, the hexaacyl *E. coli* lipid A model used can be exchanged for a heptaacyl *S. minnesota* lipid A model without significant effects on the overall model conformation. Such a model modification has not been calculated, but since the hydroxymethyl groups of the GlcN II moieties of the *E. coli* and the *S. minnesota* models show very similar orientations (13, 16), our assumption should hold true. It is also obvious that some other types of O-specific chains (2) should be compatible with the calculated model, since such O-specific chain structures differ from the one used in this study only by replacement of the side-chain Abe for tyvelose and paratose, respectively (3, 11). Finally, since it is reported that the *E. coli* R1, R2, R3, and R4 core oligosaccharides show conformations similar to that of the *S. typhimurium* core (11), it can be argued that these LPS portions are interchangeable in the calculated model without significant changes in the overall conformation. In conclusion, the calculated model is probably compatible with a wide range of structural modifications.

From the calculated models, four structural domains can be distinguished: lipid A, the inner core, the outer core, and the O-specific chain (Fig. 4). Therefore, such a subdivision of LPS into regions can be based not only on primary chemical structural data but also on the conformational properties (overall shape and flexibility) of LPS. In this context it is noteworthy that the inner core region in the calculated models forms a compact structural element that shows only minor flexibility and that has an anisotropic shape similar to that of the lipid anchor. Therefore, it can be speculated that the inner core plus the lipid anchor form one functional entity of LPS. On the other hand, according to our calculations, a subdivision of the inner core into KDO and heptose regions is not straightforward concerning the overall shape of the calculated model.

In the inner core and the lipid A head group regions, several charged groups are located. An inspection of the

models revealed that all phosphate groups are exposed to the surface, whereas some of the KDO carboxyl groups are buried in the inside of the molecule. Nevertheless, the lipid A phosphate groups and the inner core region represent characteristic charge patterns. It can be argued that such a charge pattern might be one of the reasons for the exceptionally strong binding affinity of LPS (not of the O-specific chain but of partial structures down to Rc and Rd) to monoclonal antibodies (7).

A rodlike overall shape has been proposed for LPS (20); more recently, other authors suggested that LPS has a heavily coiled structure (16, 28, 32). The present calculations, however, suggest that the LPS inner and outer core oligosaccharide portions are conformationally rather well defined, in contrast to the O-specific chain, which is the most flexible component within the complete LPS model. These data, together with X-ray experiments indicating a small increase in molecular extensions of S-form LPS with respect to Ra-LPS of only 1.0 to 1.4 nm (Table 1), seem to favor a heavily coiled O-specific chain. However, we do not strictly follow this line of reasoning. First, our calculations on the flexibility of the O-specific chain demonstrate that the O-specific chains are likely to bend at specific sites, namely, at the Rha-Gal and the Gal-Man linkages. Other parts of the O-specific chain appeared to be relatively conserved in their conformation, so that, on the average, significant stretches of linear or helical and few coiled sequences alternate. Thus, the O-specific chain shows some degree of order. Second, the small increase in molecular dimensions found in our experiments indicates heterogenity in LPS composition rather than a compressed and coiled O-specific chain (25).

The following considerations support this conclusion. The increase in length (ΔL) from Ra-LPS to S-form LPS is about 1.0 to 1.4 nm (Table 1). Assuming an upper limit for the membrane area (A) of a single LPS molecule of 1.50 nm^2 (13, 23), the O-specific chain volume per molecule is $\Delta L \times A =$ 1.5 to 2.1 nm^3. Since the volume for one repeating unit was evaluated to be 0.77 to 0.79 nm^3, the number of repeating units per LPS molecule would be 2 to 3. Although this value is an average value and LPS material extracted from bacteria can be assumed to consist of longer and shorter molecules (25), our example demonstrates that the X-ray experiments (16, 41) do not per se indicate long-chain LPS.

It is known from electron microscopic studies that antibody binding to the O-specific chain can appear at distances of more than 20 nm from the lipid region of the outer membrane, indicating that at least some of the O-specific chains can be stretched (34). From the dimensions of the most stretched LPS model, it can be estimated that more than 11 repeating units are required to span such a distance.

Taking all of these data and the results of our model calculations into consideration, the following model of the arrangement of LPS in the outer membrane can be proposed. The Ra-LPS portion shows a relatively well defined cylindrical overall shape, and its long axis can be assumed to run parallel to the membrane normal. The O-specific chain, however, does not represent a regular helix over longer chain distances. Furthermore, there would also be a good agreement with experimental dimensions for S-form LPS, assuming that the O-specific chain prefers conformations in which it is bent relative to the membrane normal and partially lies flat on top of the head groups of other membrane molecules, some of which lack parts of or the complete O-specific chain. The O-specific chain is flexible enough to be stretched out to significant distances into the extracellular space (Fig. 6). Since a number of longer O-specific chains may produce crossovers, a mechanically stable, feltlike network may be formed. In this way, the layer formed by the O-specific chains can function as an effective barrier against permeation of harmful substances (32).

It should be noted that the proposed outer membrane architecture does not conflict with the model favored by Labischinski et al. (16). Both models suggest irregular O-specific chain arrangements. With our model, we predict that these irregularities are not only irregularities of a single O-specific chain but may also include feltlike crossovers of several strands and chain length variations.

Sets of atomic coordinates and of glycosidic torsion angles of the models are available from the authors.

ACKNOWLEDGMENTS

This work was supported by the Deutsche Forschungsgemeinschaft.

We thank H. Bombosch for preparing drawings. We are also indebted to C. Schultz for advice and expert work in preparing the LPS structural diagram. We are grateful to E. T. Rietschel and H. Labischinski for fruitful discussions and valuable suggestions.

REFERENCES

1. **Bock, K.** 1983. The preferred conformation of oligosaccharides in solution inferred from high resolution NMR data and hard-sphere exo-anomeric calculations. Pure Appl. Chem. **55**:605–622.
2. **Bock, K., M. Meldal, D. R. Bundle, T. Iversen, P. J. Garegg, T. Norberg, A. A. Lindberg, and S. B. Svenson.** 1984. The conformation of *Salmonella* O-antigenic polysaccharide chains of serogroups A, B, and D1 predicted by semi-empirical, hard-sphere (HSEA) calculations. Carbohydr. Res. **130**:23–34.
3. **Brade, H., L. Brade, and E. T. Rietschel.** 1988. Structure-activity relationships of bacterial lipopolysaccharides (endotoxins). Zentralbl. Bakteriol. Parasitenkd. Infektionskr. Hyg. Abt. 1 Orig. Reihe A **268**:151–179.
4. **Brandenburg, K., and U. Seydel.** 1984. Physical aspects of structure and function of membranes made from lipopolysaccharides and free lipid A. Biochim. Biophys. Acta **775**:225–238.
5. **Cambridge University Press.** 1990. Crystal structure search and retrieval (CSSR). Cambridge University Press, Cambridge.
6. **Cygler, M., D. R. Rose, and D. R. Bundle.** 1991. Recognition of a cell-surface oligosaccharide of pathogenic *Salmonella* by an antibody Fab fragment. Science **253**:442–445.
7. **Di Padova, F., R. Barkley, and E. Liehl.** 1991. Identification of widely cross-reactive and cross-protective anti-LPS core monoclonal antibodies, p. 118–119, abstr. 331. *In* Circulatory shock. Second International conference on Shock, June 1991. John Wiley & Sons, Inc., New York.
8. **Ferris, F. G.** 1989. Metallic ion interactions with the outer membrane of Gram-negative bacteria, p. 295–323. *In* T. J. Beveridge and R. J. Doyle (ed.), Metal ions and bacteria. John Wiley & Sons, Inc., New York.
9. **Hagler, A. T., P. S. Stern, R. Sharon, J. M. Becker, and F. Naider.** 1979. Computer simulation of the conformational properties of oligopeptides. Comparison of theoretical methods and analysis of experimental results. J. Am. Chem. Soc. **101**:6842–6852.
10. **Haishima, Y., O. Holst, and H. Brade.** 1992. Structural investigation on the lipopolysaccharide of *Escherichia coli* rough mutant F653 representing the R3 core type. Eur. J. Biochem. **203**:127–134.
11. **Jansson, P. E., R. Wollin, G. W. Bruse, and A. A. Lindberg.** 1989. The conformation of core oligosaccharides from *Escherichia coli* and *Salmonella typhimurium* lipopolysaccharides as predicted by semi-empirical calculations. J. Mol. Recogn. **2**:25–36.
12. **Kastowsky, M.** Unpublished results.

13. **Kastowsky, M., A. Sabisch, T. Gutberlet, and H. Bradaczek.** 1991. Molecular modelling of bacterial deep rough mutant lipopolysaccharide of *Escherichia coli*. Eur. J. Biochem. **197:** 707–716.
14. **Kastowsky, M., A. Sabisch, T. Gutberlet, M. von Frieling, and H. Bradaczek.** 1990. X-ray diffraction and molecular modelling of bacterial lipopolysaccharides. Acta Cryst. **A49**(Suppl.): PS.03.06.17.
15. **Kato, N., M. Ohta, N. Kido, H. Ito, S. Naito, T. Hasegawa, T. Watabe, and K. Sasaki.** 1990. Crystallization of R-form lipopolysaccharides from *Salmonella minnesota* and *Escherichia coli*. J. Bacteriol. **172:**267–280.
16. **Labischinski, H., G. Barnickel, H. Bradaczek, D. Naumann, E. T. Rietschel, and P. Giesbrecht.** 1985. High state of order of isolated bacterial lipopolysaccharide and its possible contribution to the permeation barrier property of the outer membrane. J. Bacteriol. **162:**9–20.
17. **Labischinski, H., E. Vorgel, W. Uebach, R. P. May, and H. Bradaczek.** 1990. Architecture of bacterial lipid A in solution: a neutron small-angle scattering study. Eur. J. Biochem. **190:**359–363.
18. **Leps, B., G. Barnickel, H. Bradaczek, and H. Labischinski.** 1984. Structural studies on the bacterial cell wall peptidoglycan pseudomurein. I. Conformational energy calculations on the glycan strands in C1 conformation and comparison with murein. J. Theor. Biol. **107:**85–114.
19. **Lüderitz, O., M. A. Freudenberg, C. Galanos, V. Lehmann, E. T. Rietschel, and D. H. Shaw.** 1982. Lipopolysaccharides of Gram-negative bacteria. Curr. Top. Membr. Transp. **17:**79–151.
20. **Lugtenberg, B., and L. van Alphen.** 1983. Molecular architecture and functioning of the outer membrane of *Escherichia coli* and other Gram-negative bacteria. Biochim. Biophys. Acta **737:**51–115.
21. **Metropolis, N., A. W. Rosenbluth, M. N. Rosenbluth, and A. H. Teller.** 1953. Equation of state calculations by fast computing machines. J. Chem. Phys. **21:**1087–1092.
22. **Meyer, B.** 1990. Conformational aspects of oligosaccharides. Top. Curr. Chem. **154:**141–208.
23. **Naumann, D., C. Schultz, A. Sabisch, M. Kastowsky, and H. Labischinski.** 1989. New insights into the phase behaviour of a complex anionic amphiphile: architecture and dynamics of bacterial deep rough lipopolysaccharide membranes as seen by FT-IR, X-ray, and molecular modelling techniques. J. Mol. Struct. **214:**213–246.
24. **Paulsen, H., T. Peters, V. Sinwell, R. Lebhuhn, and B. Meyer.** 1984. Bestimmung der Konformation von Tri- und Tetrasaccharidsequenzen der Core-Struktur von N-Glycoproteinen. Problem der (1-6)-glycosidischen Bindung. Liebigs Ann. Chem. **1984:**951–976.
25. **Peterson, A. A., and E. J. McGroarty.** 1985. High-molecular-weight components in lipopolysaccharides of *Salmonella typhimurium*, *Salmonella minnesota*, and *Escherichia coli*. J. Bacteriol. **162:**738–745.
26. **Pincus, M. R., A. W. Burgess, and H. A. Scheraga.** 1976. Conformational energy calculations of enzyme-substrate complexes of lysozyme. I. Energy minimization of monosaccharide and oligosaccharide inhibitors and substrates of lysozyme. Biopolymers **15:**2485–2521.
27. **Qureshi, N., K. Takayama, D. Heller, and C. Fenselau.** 1983. Position of ester groups in the lipid A backbone of lipopolysaccharides obtained from *Salmonella typhimurium*. J. Biol. Chem. **258:**12947–12951.
28. **Rietschel, E. T., L. Brade, U. Schade, U. Seydel, U. Zähringer, S. Kusumoto, and H. Brade.** 1987. Bacterial endotoxins: properties and structure of biologically active domains, p. 1–41. *In* E. Schrinner, M. H. Richmond, G. Seibert, and U. Schwartz (ed.), Surface structures of microorganisms and their interactions with the mammalian host. Verlag Chemie, Weinheim, Germany.
29. **Rietschel, E. T., H. W. Wollenweber, H. Brade, U. Zähringer, B. Lindner, U. Seydel, H. Bradaczek, G. Barnickel, H. Labischinski, and P. Giesbrecht.** 1984. Structure and conformation of the lipid A component of lipopolysaccharides, p. 187–220. *In* R. Proctor and E. T. Rietschel (ed.), Handbook of endotoxins, vol. 1. Chemistry of endotoxins. Elsevier/North-Holland Biomedical Press, Amsterdam.
30. **Rozalski, A., L. Brade, H. M. Kuhn, H. Brade, and P. Kosma.** 1989. Determination of the epitope specificity of monoclonal antibodies against the inner core region of bacterial lipopolysaccharides by use of 3-deoxy-D-manno-octulosonate-containing synthetic antigens. Carbohydr. Res. **193:**257–270.
31. **Schlenkrich, M., K. Nicklas, J. Brickmann, and P. Bopp.** 1990. A molecular dynamics study of the interface between a membrane and water. Ber. Bunsen-Ges. Phys. Chem. **94:**133–145.
32. **Seltmann, G.** 1990. Significance of composition and structure of the enterobacterial outer membrane to the transport of desired and undesired substances and its inhibition. Acta Biotechnol. **10:**107–115.
33. **Seydel, U., K. Brandenburg, H. J. Koch, and E. T. Rietschel.** 1989. Supramolecular structure of lipopolysaccharide and free lipid A under physiological conditions as determined by synchrotron small-angle X-ray diffraction. Eur. J. Biochem. **186:** 325–332.
34. **Shands, J. W., J. A. Graham, and K. Nath.** 1967. The morphologic structure of isolated bacterial lipopolysaccharide. J. Mol. Biol. **25:**15–21.
35. **Shelling, J. G., D. Dolphin, P. Wirz, R. E. Cobbledick, and F. W. B. Einstein.** 1984. 2′-Fluoromaltose: synthesis and properties of 4-O-(2-deoxy-2-fluoro-alpha-D-glucopyranosyl) D-glucopyranose, and the crystal structure of 2,3-di-O-acetyl-1,6-anhydro-4-O-(3,4-tri-O-acetyl-2-deoxy-2-fluoro-alpha-D-gluco-pyranosyl)-beta-D-glucopyranose. Carbohydr. Res. **132:** 241–259.
36. **Stuike-Prill, R., and B. Meyer.** 1990. A new force-field program for the calculation of glycopeptides and its application to a heptacosapeptide-decasaccharide of immunoglobulin G1. Eur. J. Biochem. **194:**903–919.
37. **Svensson, G., J. Albertsson, C. Svensson, G. Magnusson, and J. Dahmen.** 1986. X-ray crystal structure of galabiose, O-alpha-D-galactopyranosyl-(1- 4)-D-galactopyranose. Carbohydr. Res. **146:**29–38.
38. **Thoergensen, H., R. U. Lemieux, K. Bock, and B. Meyer.** 1982. Further justification for the exo-anomeric effect. Conformational analysis based on nuclear magnetic resonance spectroscopy of oligosaccharides. Can. J. Chem. **60:**44–57.
39. **van der Ploeg, P., and H. J. C. Berendsen.** 1982. Molecular dynamics simulation of a bilayer membrane. J. Chem. Phys. **76:**3271–3276.
40. **von Frieling, M.** 1990. Strukturuntersuchungen an synthetischen Lipiden und bakteriellen Endotoxinen. Eine Röntgenbeugungsstudie an Langmuir-Blodgett Filmen mit direkter Elektronendichteberechnung. Thesis, Freie Universität Berlin, Berlin.
41. **Wawra, H., H. Buschmann, H. Formanek, and S. Formanek.** 1977. Structural investigations on lipopolysaccharides of mutants SF1111 and R595 SF1176 of *Salmonella minnesota*. Z. Naturforsch. **34c:**171–177.
42. **Westphal, O.** 1984. Introduction: short history, questions and outlook, p. 17–23. *In* R. Proctor and E. T. Rietschel (ed.), Handbook of endotoxins, vol. 1. Chemistry of endotoxins. Elsevier/North-Holland Biomedical Press, Amsterdam.
43. **Yadav, J. S., H. Labischinski, G. Barnickel, and H. Bradaczek.** 1981. Quantum chemical studies on the conformational structure of bacterial peptidoglycan. I. MNDO calculations on the glycan moiety. J. Theor. Biol. **88:**441–457.
44. **Zähringer, U., B. Lindner, U. Seydel, E. T. Rietschel, H. Naoki, F. M. Unger, M. Imoto, S. Kusumoto, and T. Shiba.** 1985. Structure of de-O-acylated lipopolysaccharide from the *Escherichia coli* mutant strain F 515. Tetrahedron Lett. **26:**6321–6324.